Journal of Sound and Vibration (1997) **203**(2), 352–357

TRANSVERSE VIBRATIONS OF POLYGONAL PLATES OF DISCONTINUOUSLY VARYING THICKNESS WITH A FREE, CONCENTRIC CIRCULAR EDGE

D. V. Bambill

Department of Engineering, Universidad Nacional del Sur, 8000-Bahia Blanca, Argentina

V. Sonzogni

INTEC (CONICET) and Facultad Regional Santa Fe-UTN, 3000-Santa Fe, Argentina

and

P. A. A. Laura

Institute of Applied Mechanics (CONICET) and Department of Engineering, Universidad Nacional del Sur 8000-Bahia Blanca, Argentina

(*Received* 17 *May* 1996, *and in final form* 12 *September* 1996)

1. INTRODUCTION

The present study deals with the determination of the fundamental frequency of vibration of simply supported and clamped plates of regular polygonal shape with a free, concentric circular perforation; see Figure 1. It is assumed that the thickness varies in a discontinuous fashion in the circular annular subdomain enclosing the hole. This portion may be made of a dissimilar material. Two independent approaches are followed in order to determine the fundamental eigenvalues:

(1) By conformally transforming the given configuration in the z-plane onto circular, concentric regions in the ξ-plane and making use of the Rayleigh-Ritz method to obtain the frequency equation [1, 2]. The methodology is applicable in the case of configurations with several axes of symmetry with a concentric cut-out.

(2) By the finite element algorithmic procedure using a well known finite element code [3].

2. APPROXIMATE ANALYTICAL SOLUTION

If one makes use of the classical theory of vibrating plates, the normal modes of transverse vibration of the system shown in Figure 1 are governed by the functional [4].

$$J(W) = D_0 \iint_{P_0} \left\{ \left(\frac{\partial^2 W}{\partial x^2} + \frac{\partial^2 W}{\partial y^2} \right)^2 - 2(1-\mu) \left[\frac{\partial^2 W}{\partial x^2} \frac{\partial^2 W}{\partial y^2} - \left(\frac{\partial^2 W}{\partial x \partial y} \right)^2 \right] \right\} \mathrm{d}x\, \mathrm{d}y$$

$$- D_0 \iint_{P_2} \left\{ \left(\frac{\partial^2 W}{\partial x^2} + \frac{\partial^2 W}{\partial y^2} \right)^2 - 2(1-\mu) \left[\frac{\partial^2 W}{\partial x^2} \frac{\partial^2 W}{\partial y^2} - \left(\frac{\partial^2 W}{\partial x \partial y} \right)^2 \right] \right\} \mathrm{d}x\, \mathrm{d}y$$

$$+ D_1 \iint_{P_1} \left\{ \left(\frac{\partial^2 W}{\partial x^2} + \frac{\partial^2 W}{\partial y^2} \right)^2 - 2(1-\mu) \left(\frac{\partial^2 W}{\partial x^2} \frac{\partial^2 W}{\partial y^2} - \left(\frac{\partial^2 W}{\partial x \partial y} \right)^2 \right] \right\} \mathrm{d}x\, \mathrm{d}y$$

0022–460X/97/220352 + 06 $25.00/0/sv960816

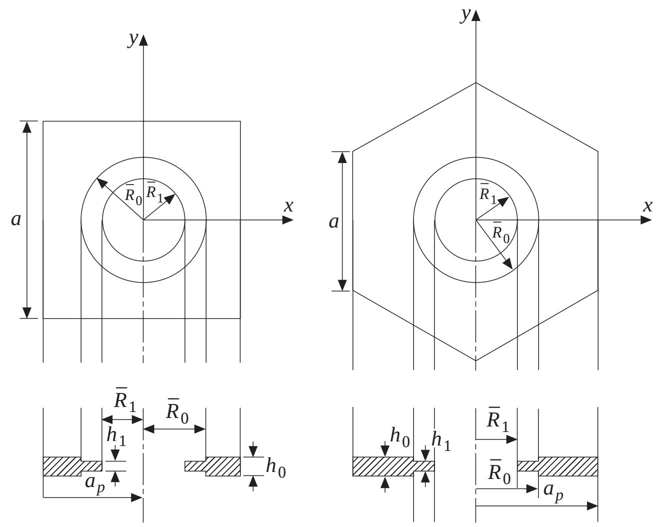

(a) (b)

Figure 1. Plates of regular polygonal shape with a free, concentric circular edge: (a) square plate, (b) hexagonal plate.

$$-\left(\rho h_0\omega^2 \iint_{P_0} W^2\,\mathrm{d}x\,\mathrm{d}y - \rho h_0\omega^2 \iint_{P_2} W^2\,\mathrm{d}x\,\mathrm{d}y + \rho h_1\omega^2 \iint_{P_1} W^2\,\mathrm{d}x\,\mathrm{d}y\right), \tag{1}$$

where W is the displacement amplitude, $D_0 = Eh_0^3/12(1-\mu^2)$, $D_1 = Eh_1^3/12(1-\mu^2)$, P_0 is the regular polygon of apothem a_p, P_2 is the circle of radius $\bar{R}_0$ and P_1 is the annular region of outer radius R_0 and inner radius R_1; see Figure 1. Clearly if the annular region P_2 is made of a different material characterized by E_1, μ_1 and ρ_1 one simply takes this into account in the corresponding expressions appearing in equation (1).

In the case where the outer boundary is simply supported the boundary conditions at the outer edge are

$$W(x, y)) = M_n(x, y) = 0, \tag{2a, b}$$

where M_n is the bending moment normal to the edge. On the other hand, when the outer edge is clamped one has

$$W(x, y) = (\partial W/\partial n)(x, y) = 0 \tag{3a, b}$$

at the outer edge.

Since complying with the natural boundary conditions at the free circular edge will be extremely complicated, use will be made of polynomial coordinate functions which satisfy only the essential boundary conditions at the outer edge.†

A regular polygonal shape in the z-plane is transformed onto a unit circle in the ξ-plane by means of [2]

$$z = a_p A_s \sum_{k=0}^{\infty} (-1)^k a_k \xi^{ks+1}, \qquad \xi = r\,\mathrm{e}^{\mathrm{i}\theta}, \tag{4}$$

† This is also the case with condition (2b) at the outer edge.

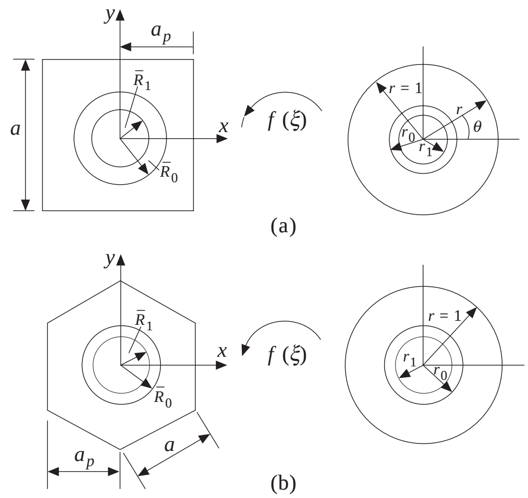

Figure 2. Approximate conformal mapping of the configurations under study: (a) square plate, (b) hexagonal plate. On the left are the z-plane configurations, on the right are the ξ-plane shapes.

where s is the degree of the polygon, A_s is the coefficient [2], and $a_k = a_{k-1}[(k-1)k+1][(k-1)s+2]/[ks(ks+1)]$, and $a_0 = 1$. Expression (4) transforms also, approximately, the circular subdomain of radius $\bar{R}_0$ if $\bar{R}_0 \ll a_p$.

The corresponding approximate radius in the ξ-plane is [1], see Figure 2,

$$r_0 \simeq \bar{R}_0 / A_s a_p, \tag{5a}$$

since $r \ll 1$. Similarly,

$$r_1 \simeq \bar{R}_1 / A_s a_p. \tag{5b}$$

The following coordinate functions have been used in the present investigation: simply supported outer edge,

$$W(r) = A_1(1-r^2) + A_2(1-r^2)r^2 + A_3(1-r^2)r^4; \tag{6}$$

clamped outer edge,

$$W(r) = A_1(1-r^2)^2 + A_2(1-r^2)^2 r^2 + A_3(1-r^2)^2 r^4. \tag{7}$$

These approximations are substituted in the governing functional (1) once transformation is performed into the ξ-plane. The evaluation of the integrals is performed by means of MATHEMATICA. Minimizing the functional with respect to the A_is one finally sets up a frequency determinant whose lowest root is the fundamental frequency coefficient $\Omega_1 = \sqrt{\rho h_0 / D_0}\, \omega_1 a^2$, where a is the side of the polygon.

3. FINITE ELEMENT DETERMINATIONS

The numerical results have been obtained using the SAMCEF finite element code using hybrid elements of triangular and rectangular shape (elements type 55 and 56 of the SAMCEF Library). The number of elements varied in accordance with the plate configuration; for instance in the case of hexagonal plates one sixth of the domain was subdivided into 588 elements with 2659 degrees of freedom.

4. NUMERICAL RESULTS

All calculations were performed for $\mu = 0{\cdot}30$. Table 1 depicts fundamental frequency coefficients for simply supported and clamped square plates for several values of $\bar{R}_1/a_p$ and $\bar{R}_0/a_p$. The finite element results (presumably of considerable higher accuracy) are lower than the approximate analytical results.

The agreement is closer in the case of a clamped outer edge due to the satisfaction of the governing essential boundary conditions at the outer edge. It is important to point out that present analytical results are in good agreement with those obtained in reference [5].

Table 2 shows fundamental eigenvalues for simply supported and clamped hexagonal plates. The agreement between finite element values and the approximate, analytical results is now better than in the case of Table 1. This is due to the fact that the approximations involved when transforming the circular boundaries of the discontinuity and of the hole

TABLE 1

Comparison of fundamental frequency coefficients in the case of a square plate: A, simply supported case; B, clamped case

	$R_1 = \bar{R}_1/a_p$	$R_0 = \bar{R}_0/a_p$		Values of $\Omega_1 = \omega_1 a^2\sqrt{\rho h_0/D_0}$ Thickness variation ($h_1/h_0 = \alpha$) 1	0·90	0·80	1·10	1·20
A	0·05	0·1	(1)	19·90	19·88	19·87	19·93	19·97
			(2)	19·67	19·63	19·59	19·71	19·75
		0·2	(1)	–	19·81	19·75	20·03	20·18
			(2)	–	19·54	19·39	19·78	19·86
		0·3	(1)	–	19·69	19·53	20·17	20·46
			(2)	–	19·41	19·13	19·87	20·04
	0·1	0·2	(1)	19·89	19·91	19·86	20·09	20·23
			(2)	19·53	19·39	19·26	19·66	19·77
		0·3	(1)	–	19·78	19·63	20·24	20·52
			(2)	–	19·26	19·00	19·75	19·94
	0·2	0·3	(1)	20·30	20·16	20·06	20·50	20·73
			(2)	19·28	19·08	18·93	19·48	19·70
		0·4	(1)	–	19·98	19·74	20·69	21·13
			(2)	–	18·95	18·67	19·60	19·93
	0·3	0·4	(1)	20·84	20·64	20·50	21·12	21·46
			(2)	19·48	19·30	19·17	19·70	19·95
B	0·05	0·1	(1)	36·37	36·35	36·34	36·42	36·48
			(2)	35·79	35·72	35·64	35·85	35·91
		0·2	(1)	–	36·24	36·18	36·55	36·77
			(2)	–	35·57	35·37	35·91	36·02
		0·3	(1)	–	36·11	35·95	36·70	37·07
			(2)	–	35·42	35·13	35·99	36·21
	0·1	0·2	(1)	36·70	36·59	36·54	36·85	37·06
			(2)	35·67	35·48	35·31	35·84	36·00
		0·3	(1)	–	36·45	36·31	37·02	37·39
			(2)	–	35·35	35·11	35·90	36·14
	0·2	0·3	(1)	38·06	37·91	37·82	38·31	38·62
			(2)	36·30	36·17	36·11	36·48	36·69
		0·4	(1)	–	37·83	37·80	38·45	38·94
			(2)	–	36·14	36·15	36·50	36·78
	0·3	0·4	(1)	40·90	40·90	41·04	41·04	41·30
			(2)	39·14	39·23	39·42	39·15	39·23

(1) Analytical solution. (2) Numerical solution (finite element method).

TABLE 2

Comparison of fundamental frequency coefficients in the case of a hexagonal plate: A, simply supported case; B, clamped case

			Values of $\Omega_1 = \omega_1 a^2\sqrt{\rho h_0/D_0}$ Thickness variation (α)				
R_1	R_0		1	0·90	0·80	1·10	1·20
0·05	0·1	(1)	7·173	7·166	7·162	7·184	7·198
		(2)	7·114	7·097	7·080	7·128	7·141
	0·2	(1)	–	7·137	7·114	7·221	7·279
		(2)	–	7·061	7·001	7·156	7·189
	0·3	(1)	–	7·090	7·029	7·272	7·381
		(2)	–	7·011	7·902	7·200	7·270
0·1	0·2	(1)	7·206	7·176	7·157	7·247	7·297
		(2)	7·057	7·003	6·950	7·107	7·151
	0·3	(1)	–	7·127	7·070	7·302	7·409
		(2)	–	6·956	6·854	7·149	7·227
0·2	0·3	(1)	7·332	7·276	7·238	7·406	7·495
		(2)	6·968	6·896	6·836	7·049	7·132
	0·4	(1)	–	7·208	7·116	7·481	7·646
		(2)	–	6·846	6·742	7·099	7·230
0·3	0·4	(1)	7·549	7·469	7·418	7·654	7·784
		(2)	7·069	7·003	6·959	7·153	7·250
0·05	0·1	(1)	12·836	12·826	12·822	12·852	12·876
		(2)	12·749	12·721	12·692	12·773	12·793
	0·2	(1)	–	12·787	12·761	12·904	12·986
		(2)	–	12·674	12·594	12·809	12·854
	0·3	(1)	–	12·736	12·674	12·959	13·094
		(2)	–	12·627	12·515	12·857	12·950
0·1	0·2	(1)	12·956	12·915	12·895	13·017	13·093
		(2)	12·710	12·639	12·575	12·780	12·843
	0·3	(1)	–	12·862	12·809	13·078	13·216
		(2)	–	12·600	12·510	12·818	12·919
0·2	0·3	(1)	13·467	13·409	13·389	13·558	13·677
		(2)	12·979	12·933	12·916	13·047	13·129
	0·4	(1)	–	13·386	13·378	13·606	13·789
		(2)	–	12·931	12·940	13·064	13·174
0·3	0·4	(1)	14·551	14·562	14·623	14·591	14·678
		(2)	14·120	14·162	14·246	14·117	14·146

(1) Analytical solution· (2) Numerical solution (finite element method).

are now closer than in the case of the square plate since equation (4) converges faster for $r \ll 1$.

In general the approximation yields accurate eigenvalues, from an engineering viewpoint, for $\bar{R}_0/a_p < 0{\cdot}5$.

From the analysis of Tables 1 and 2 one concludes that a dynamic stiffening effect takes place for all the configurations.

ACKNOWLEDGMENTS

The present study has been sponsored by CONICET Research and Development Program (PIA 1996-1997) and by Secretaría General de Ciencia y Technología of Universidad Nacional del Sur (Program Director: Professor R. E. Rossi).

The authors are indebted to Professor R. H. Gutierrez for his valuable advice regarding the approximate analytical solution presented in this paper and to one of the referees of the present publication for his very constructive criticism.

REFERENCES

1. P. A. A. LAURA, E. ROMANELLI and M. J. MAURIZI 1972 *Journal of Sound and Vibration* **20**, 27–38. On the analysis of waveguides of doubly-connected cross-sections by the method of conformal mapping.
2. R. SCHINZINGER and P. A. A. LAURA 1991 (*Conformal Mapping*: *Methods and Applications*). Amsterdam, The Netherlands: Elsevier.
3. SAMCEF User's Manuals, V. 5.1. 1994. Belgium: Samtech and University of Liege.
4. S. TIMOSHENKO and S. WOINOWSKY-KRIEGER 1959 (*Theory of Plates and Shells*). New York, N.Y.: McGraw Hill.
5. P. A. A. LAURA, R. H. GUTIERREZ, V. SONZOGNI and S. IDELSOHN 1996 *Journal of Sound and Vibration* **199,** 704–710. Transverse vibrations of rectangular plates of non-uniform thickness with a free, concentric circular hole.